



# Study of Image-Based Finite Element Model for Predicting the Biomechanical Properties of Femur Bone: A Review

Rahul Gujar<sup>1</sup> · Hemant Warhatkar<sup>1</sup> · Amit Kale<sup>2</sup>

Received: 22 October 2022 / Accepted: 4 April 2023 / Published online: 12 April 2023  
© The Institution of Engineers (India) 2023

**Abstract** This paper aims to provide insight into the current state-of-the-art literature available for investigating the biomechanical properties of the femur bone. Furthermore, this comprehensive review has addressed some challenges when predicting femur bone biomechanical properties. This review also includes an in-depth discussion on the essential biomechanical properties of femur bone obtained using different imaging techniques, failure and loading criteria, etc. Further, quantitative data on deviations in biomechanical properties estimated using experimental and numerical methods from the available literature have presented and discussed. In addition, the study has demonstrated the non-invasive and non-destructive computed tomography scan technique to create a three-dimensional finite element model for predicting the biomechanical properties. This paper will help to understand the clinical issues and other challenges related to estimating the biomechanical properties, such as the effect of different bone inclinations, failure criteria and related fracture risk.

**Keywords** Biomechanical properties · Finite element model · Femur bone · Computed tomography

## Introduction

Femur bone is a natural composite of hard tissues supporting the soft muscles of the human body. On a weight basis, it contains approximately 30% organic, 60% inorganic components and 10% water [1]. Femur is the longest, largest and strongest bone in the body as shown in Figure 1 [2]. Femur bone is subjected to mechanical loads during physiological activities that influence their biomechanical properties [3]. Nowadays, image-based modelling technique is used to predict the biomechanical behaviour of femur bone. However, accurate image-based finite element modelling is still challenging [4, 5]. The femur bone has different mechanical properties in the longitudinal and transverse directions while loaded along the different directions [6]. Thus, the subject-specific biomechanical properties of femur bone are vital for developing new biomaterials for bone implants and fixation. The biomechanical properties also depend on the load acting at the hip joint during various human activities such as sitting, staircase climbing, running, standing, athletics activities, daily workout and accidental injuries [7]. According to the data presented on the number of hip fractures occurring annually in the world, it will increase from 1.66 million in 1990 to 6.26 million in 2050 [8]. In 2010, the European Union reported 620,000 hip fractures. Hence, the economic burden of fracture incidents was estimated at €37 billion. The expenditure is expected to increase by 25% in 2025 [9]. In India, according to the report in 2004, the estimated osteoporotic hip fracture incidences were 6,00,000 per year and are expected to increase significantly by 2026 [10].

---

✉ Rahul Gujar  
rahulgajar.research@gmail.com

<sup>1</sup> Department of Mechanical Engineering, Dr.Babasaheb Ambedkar Technological University, Lonere, Raigad, Maharashtra, India

<sup>2</sup> Department of Orthopaedics, Dr.D.Y.Patil Medical College, Hospital and Research Centre, Pimpri-Chinchwad, Pune, Maharashtra, India

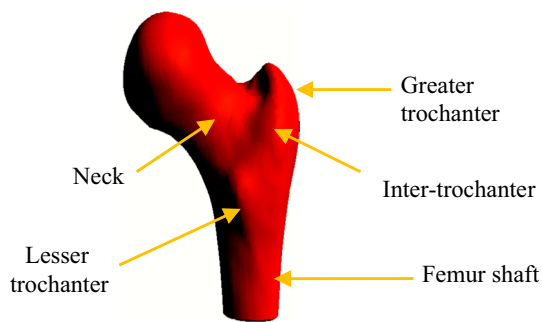


**Fig. 1** Anatomy of the femur bone [2]

## Biomechanical Properties

Bone is made up of a natural combination of composite materials. Consequently, the studies and knowledge of its mechanical properties are essential for understanding the fracture mechanism and its patterns. It also assists in the design and development of implants, prosthetics, fixation, and the diagnosis of bone-related issues. Thus, this review has discussed some critical biomechanical properties like mass density, elastic modulus, stress-strain characteristics and fracture load.

### Mass Density

Mass density is an important biomechanical property of femur bone. It will decide the percentage porosity/quality of femur. Consequently, it predicts the condition of femur bone such as osteoporosis, osteopenia or healthy. The femur bone mass density varies with age, gender, birthhood conditions, eating habits etc. In the available literature, mass density is estimated by linear and power models in terms of Hounsfield unit (HU) [11]. Adams et al. [12] estimated mass density using computed tomography and the conventional Archimedes technique. In some studies, the researchers used the available mathematical models to estimate the density of femur bone [13, 14]. Ducheynet et al. [15] used the conventional method, defined as the bonesample weight divided by the total sample volume, to determine the mean apparent mass density of intracondylar femur bone. Further, it is used to estimate mechanical properties. Generally, in stance and fall configuration, the fracture occurred in neck-head region of femur bone. Therefore, it is required to focus on evaluating density at this region [2]. It was also observed that the lower mass density distributed in neck-head region of femur bone. Moreover, Morgan et al. [16] have studied the site dependent apparent mass density. The sites such as the vertebra, tibia, greater trochanter and femoral neck were selected. The obtained range of apparent mass density was reported as 260–750 kg/m<sup>3</sup> at the femoral neck region [2, 16]. Some researchers used the linear relationship between

**Table 1** Various mathematical (linear/power) models to calculate elastic modulus

Mathematical model	Equations	Reference
Power model	$E = 6.850 * \rho^{1.49}$	Morgan et al. [16]
Power model	$E = 8.920 * \rho^{1.83}$	Morgan et al. [16]
Linear model	$E = -331 + 4.56\rho$	Rho et al. [30]
Power model	$E = 0.58 * \rho^{1.30}$	Rho et al. [30]
Linear model	$E = -13.43 + 14.261\rho$	Lotz et al. [41]
Power model	$E = 1904 * \rho^{1.83}$	Wirtz et al. [42]

apparent mass density and Hounsfield unit (HU) for femoral bone and determined the relative error as 18.3–44.9%. These studies signify the need for further improvements to estimate mass densities more accurately [17–19].

### Elastic Modulus

It decides the bone quality in terms of elastic properties and strength. In humans, if a bone is osteoporotic, the elastic modulus is lower than the healthy bone. The healthy femur has an elastic modulus ranging from 9 to 20 GPa [20–23] and changes from region to region of the bone. Hence elastic modulus of the femur bone is a heterogeneous and non-linear [13, 24]. However, in the literature, many authors considered linear elastic modulus [25–29]. It has limited accuracy in predicting the other dependent biomechanical properties using finite element analysis (FEA). Few studies have reported various techniques such as ultrasonic [30], nano-indentation [20, 31, 32], CT scan image-based [2, 33, 34], mathematical models (linear/power) [11, 35], electronic speckle pattern interferometry (ESPI) [36] to estimate the elastic properties. Whereas, Sitzler et al. [37] experimentally determined Young's modulus of femur bone by using a compression test. Further, it was compared with Young's modulus calculated from density-elasticity relationship available in the literature and found significant deviation. In addition, Cyganik et al. [38] carried out experimental and numerical analyses of trabecular bone to estimate elastic modulus. Niebur et al. [39] have also performed high-resolution finite element analysis of bovine trabecular bone to estimate the modulus of elasticity as  $18.7 \pm 3.7$  GPa. Wherein, Brennan et al. [40] have calculated the average modulus of elasticity as  $20.78 \pm 2.4$  GPa by using nano-indentation test. Table 1 gives the various mathematical (linear/power) models to calculate the elastic modulus of the femur bone.

### Fracture Risk/Load

It is an essential biomechanical property of femur bone which shows the mechanical ability to sustain the load before fracture. The femur bone is subjected to compressive

loading in stance configuration in various physiological states such as jogging, slow/fast walking, athletics exercises and sports. The femur bone loadings are static, quasi-static or dynamic, depending on various types of hip joint movement and its mechanics. In addition, the bone fracture load magnitude is influenced by different displacement rates and inclination angles during hip joint positions. In the available literature, authors have used a wide range of displacement rates as 0.1–42.33 mm/s [43–47] and inclination from 0° to 20° [13, 24, 25, 27, 29, 48–56] to determine biomechanical properties of femur bone. The inclination angle is measured between the mechanical and anatomical axis of femur bone fixed at the distal end. Furthermore, some studies have also been conducted to evaluate the biomechanical properties of animal species. [2, 40, 57]. However there is a need to focus on the accuracy and validation of the biomechanical properties using advanced techniques. Yashibash et al. [58] have discussed the FE model of only two femurs to predict computed yield load. The authors used and compared four different criteria: Drucker–Prager, Von-mises, maximum principal stress and strain. Moreover, the isotropic and anisotropic yield criterion-based FE model was compared with experimental results. In a reported study, Miura et al. [59] compared the fracture load on fresh frozen cadaver femurs by using a CT-based FEA model and mechanical testing. The purpose of Bessho et al. [60] study was to create the simulation FE model to evaluate the strength of femur bone. Moreover, Ota et al. [25] have worked on the fracture simulation of the femur bone using FEA and compared it with experimental results. Schileo et al. [61] determined the femur bone strength from the computed tomography (CT) based finite element (FE) model. FE predicted fracture loads and locations correlated with experimental results under stance and fall configurations. Schileo et al. [62] have experimentally predicted the failure loads on femur, similar loads applied to the FE models for computing the fracture risks and compared to the experimental test results. Keyak et al. [48] have studied in situ and in vitro CT scan-based FE models for determining fracture loads in the human cadaveric femur bone. In FEA, the femur bone was inclined at 20° [60] with a loading axis under the stance configuration. These methods have shown a deviation in fracture loads of 13.3% and 5.2% in each male and female cadaveric femur bone, respectively. However, there is a scope for validation on an experimental basis. Hambli et al. [13, 49] and Bettamer et al. [50] have performed the FE and experimental analysis on femur bone specimens to predict the failure loads with their patterns. Besides, some studies have analysed the femur bone under single-legged stance configuration within the coronal plane [24, 25, 48, 50, 51, 63]. Whereas, Hambli et al. [49] has applied a slow compressed load at 20 mm/min, and Bettamer et al. [51] have applied at 2 mm/min on the femur bone until fracture. Liebl et al. [52] predicted the

fracture load of femur bone under stance and fall configuration. In this study, the multi-detector computed tomography (MDCT) imaging method was used to create a 3D model for FEA. After that, FE model was compared and validated with the experimental method. In stance configuration, the femur bone was placed with an inclined angle of 7° at 5 mm/min. In addition, for fall, the femur bone was placed with inclination angle of 30° to the horizontal plane, internally rotated by 15° and loaded at 5 mm/min. However, Sas et al. [24] have proposed the voxel-based FE model to assess the strength of healthy and metastatic proximal femurs. Despite several pieces of literature available on fracture analysis of femur bone using FEA, there is still a scope to study the advanced instrumentation for accurate prediction of femur bone fracture load. Snyder, et al. [11] have performed experimental analysis using three points bending at a displacement rate of 5 mm/min, whereas Cyganik et al. [38] carried out the experimental analysis of bone with a compressive test at the displacement rate of 0.5 mm/min. The load range was from 0 to 2000 N with every 100 N force of increment. Keyak [64], Gilchrist, et al. [65], Zani, et al. [66] have studied the effect of load direction on fracture force and obtained data on hip fracture risk. Cadaveric femurs were tested at different loading angles such as 0°, 15° and 30°, representing a fall on the hip to failure at a displacement rate of 100 mm/sec. It was found that the failure load decreased by 24% as the loading angle. In another study, experimental analysis was carried out in quasi-static and dynamic loading conditions [67]. In some studies, the authors have used different techniques such as grid-based gauges, high-speed cameras and strain gauges to analyse the fracture mechanisms and estimate the fracture load (FL) and biomechanical behaviour [67–71]. Keyak et al. [72] have studied the femoral fracture loads for two load configurations, such as during single-limb stance and fall under impact loading. In some studies, the femur bone specimens were tested at displacement rates of 0.2 mm/sec and 2 mm/sec, respectively [47, 58, 61, 68, 73–76], and bone inclination from 0° to 20° [13, 24, 25, 48–53]. The inclination angle is measured between the mechanical and anatomical axis of femur bone fixed at the distal end. Table 2 shows the summary of femur bone fracture under compressive loading.

Thus, a study should focus on the effect of different inclination angles and displacement rates on fracture risk and failure patterns of femur. Besides, fractures from traumatic injuries are likely to cause disability and loss of work efficiency. These critical health issues added, in general, to the socio-economic burden. Hence, it is significant to address the fracture load as an essential biomechanical property of the femur bone. In orthopaedic biomechanics, an assessment of the mechanical properties of femur bone is often done using mechanical in vitro experimentation [78]. Mechanical properties of the bones and implant devices are the area of

**Table 2** Summary of femur bone fracture under compression loading

Failure criteria	Fracture load (N)		Bone inclination ( $\theta^\circ$ )	Displacement rate (mm/s)	Deviation (%)	Reference
	Expt.	FEM				
Simple principal stress	8400	2000	8	0.5	76.19	Ota et al. [25]
Max. principal stress	4743	5440	7	0.083	14.7	Liebl et al. [52]
Max. principal strain	4743	4968	7	0.083	4.7	Liebl et al. [52]
Drucker–Prager	3436	4520	20	0.083	31.56	Miura et al. [59]
Drucker–Prager	3800	4400	20	0.0083	15.78	Bessho et al. [60]
Max. principal strain	6894	6050	8	2	12.25	Schileo et al. [61]
Max. principal strain	9212	7752	8	20	15.85	Schileo et al. [61]
Max. principal strain	7375	6565	8	–	10.98	Larrainzar-Garjijo et al. [77]

interest for clinicians and engineers in determining clinical injury patterns and orthopaedic pathological conditions.

### Stress–Strain Characteristics

In macroscopic structural analysis, the ultimate strength of femur bone is decided by its stress-strain characteristics. The femur bone material has anisotropic and heterogeneous behaviour. Due to this, it is challenging to predict accurate stress-strain characteristics under different loading and directions, including with the mechanics of the hip bone. These biomechanical characteristics have been used to design and develop subject-specific implants and fixations. Many authors have studied the stress-strain behaviour of hip bone under stance and fall configurations [48–56, 58–62]. Wherein researchers have considered experimental and finite element methods, there is still a scope to focus on the accuracy of the FE model to estimate stress-strain characteristics. For this, Taddei et al. [79] proposed a material mapping strategy to predict the strain accuracy of the femur FE model and compared it with the experimental method. The authors used Bonemat software to estimate Young's modulus in this study. Further, these moduli were used to obtain the strain in FEM. The linear regression coefficient of FE results was increased from 0.69 to 0.79. In addition, the average error decreased from 45.1 to 31.3%, and the peak error decreased from 228 to 134% of the maximum measured strain. Whereas, Lengsfeld et al. [80] have performed the geometry-based and voxel-based FE analysis of femur bone to estimate strain and stress. The obtained results were compared with the experimental method. In this study, the load was applied at 0.7 mm/min with a step load of 100 N till 2000 N was reached. The correlation coefficient ranged from 0.91 to 0.94. Further, Painkra et al. [53] showed a significant deviation of 30–47% by using the isotropic and anisotropic femur models, which calculated von-mises stress and strain under different loading configurations at 0°, 15° and 20°, respectively. The study obtained the maximum stresses between 29.649–49.823 MPa and 15.938–23.218 MPa for

the anisotropic and isotropic femur models. Similarly, the maximum strains obtained were between 0.00237–0.00408 and 0.00133–0.00290 for the anisotropic and isotropic models, respectively. A similar study by Kumar et al. [81, 82] was carried out on stress analysis using ANSYS 14.0. The results of von-mises stresses were found in the range of 28.85–62.22 MPa. In this, the authors considered the behaviour of the femur bone under different physiological activities such as standing, walking, jumping and running. Chethan et al. [54] have determined the von-mises and maximum principal stresses in human long and short femur bone. Similarly, Dey et al. [83] calculated von-mises stresses under axial and bending load applications using a 3D scan-based FE model. Fonseca et al. [26] have achieved the maximum stress value of 22.60 MPa by using an isotropic and orthotropic human femur material model. However, Reddy et al. [84] obtained stresses in the range of 24.1–65.6 MPa, corresponding to the age of persons ( $n = 10$ ) between 27 and 84 years. Whereas another study has reported the peak stress as 10.2 MPa using computed tomography (CT) scan-based FE model [5]. Niebur et al. [39] have determined the stresses as  $20.62 \pm 1.06$  MPa in bovine tibia specimens using FE model. Besides, Antonio et al. [55] have used the isotropic and orthotropic FE model of femur bone. The study obtained the maximum stress values of 17.95 MPa and 17.49 MPa and maximum strain values of 0.0020 and 0.0022 for the isotropic and orthotropic material model approach, respectively. The results showed the negligible influence of the different material models regarding the maximum stress and strain values [56, 85]. Some other studies also considered the linear and isotropic material properties of femur bone [25–29, 63]. Thus, the available literature does not incorporate the different loading scenarios for the femur bone specimen. It adds value to the biomechanical studies of femur bone. It also investigates the influence of different bone inclinations and displacement rates on the stress-strain state under compressive stance loading configuration. Further, there is still a need to validate the FE modelling technique with the golden method to measure strain using an electrical resistance strain

gauge (SG). Levadnyi et al. [27] have considered the wide range of femur bone inclination ( $0^{\circ}$ – $20^{\circ}$ ) and loaded at 10 mm/min under compression. In this study, the authors experimentally tested synthetic artificial femur bone to obtain strain and stiffness and compared it with FEA. The maximum strain and stiffness results were obtained as 0.003 and 1500 N/mm, respectively. Besides this, another study on the 2D image-based FE model has been compared with digital image correlation (DIC) based experimental analysis. In addition, the authors incorporated the bone inclination at  $20^{\circ}$  in the coronal plane and a loading speed of 2 mm/min to estimate the strain and fracture load of the femoral bone. However, the strain value result showed a significant deviation between FE and the experimental method [51]. Similarly, Ota et al. [25] obtained a good correlation ( $r = 0.81$ ) between the experimental and the simulated strain values at 0.5 mm/s till the complete failure of the femoral bone. Polgar et al. [28] studied the distribution of maximum and minimum principal strains (compression and tension). Aziz et al. [29] have developed the reconstructed three-dimensional (3D) finite element model of the femur bone. In this, the estimated maximum linear strains at different locations of the femur bone. Despite this, the CT scan-based 3D model was used for FE simulation purposes, showing significant deviations in the results. Further, Mathukumar et al. [86] Schileo et al. [87] have determined the stress-strain properties on the inferior-superior and lateral-medial region of the femur bone using the FE and experimental method. Nevertheless, the study of Mathukumar et al. [86] has not included the other influencing parameters, such as bone inclination and loading rate. In addition, FEM has used material properties of the femur bone from the available literature.

### Image-Based Finite Element Analysis

Medical imaging is a well-known technique to create an image-based model to diagnose clinical issues. It is also used to generate a 3D FE model and evaluate the biomechanical properties of bone. It includes 2D and 3D imaging techniques such as X-ray, dual-energy X-ray absorptiometry (DEXA), ultrasound (US), magnetic resonance imaging (MRI), positron emission tomography (PET) and computed tomography (CT) scan. Nowadays, the CT scan imaging technique is most widely used by doctors and researchers compared to other techniques. The phrase “Computed Tomography (CT)” refers to a computer-based X-ray imaging technique in which an X-ray beam is transferred to a human/animal body to produce signals through a computer to reconstruct 2D images or slices. These slices are called tomography and enclosed with more detailed information about the internal organs than the conventional X-ray method. Image slices can either be displayed as a single or stacked together by computer

software to generate a 3D image of patient organs. Further, an image scan constructing into a virtual 3D model that can be processed through required specialized software such as Simpleware scanIP, 3D doctor, materialise mimics and 3D Slicer. These softwares were used to estimate the CT scan image-based biomechanical properties from the 3D femur model [2, 13, 25, 52, 58, 59, 61]. Figure 2 shows the steps to create FE model from CT scan images. In step 1, CT scan image data is imported into the scanIP software, and then step 2 is used to analyse and segment the CT image data for converting into a 3D geometrical model. Next, step 3 replaced the geometrical model by the generation of finite element meshes, and in step 4 the mass density and elastic modulus can be evaluated based on the greyscale of CT scan image. Finally, in step 5, the FE model is imported in the suitable analysis software, and the necessary boundary conditions are assigned to predict the biomechanical properties. It will give a noninvasive and accurate FE analysis of femur bone with multiple loading conditions.

In addition, Table 3 shows some studies on image-based finite element analysis to predict the biomechanical properties of femur bones. It incorporates detailed classification such as the loading configuration, image techniques, FE material model, bone inclination, failure criteria and finally, obtained different biomechanical properties. In this, the researchers have used the most common technique, CT scan imaging, to generate the 3D model. It included the bone inclination between  $0^{\circ}$  and  $20^{\circ}$  to investigate fracture load and stress-strain characteristics. Despite this, there is further scope to validate biomechanical properties using the image-based finite element method [88].

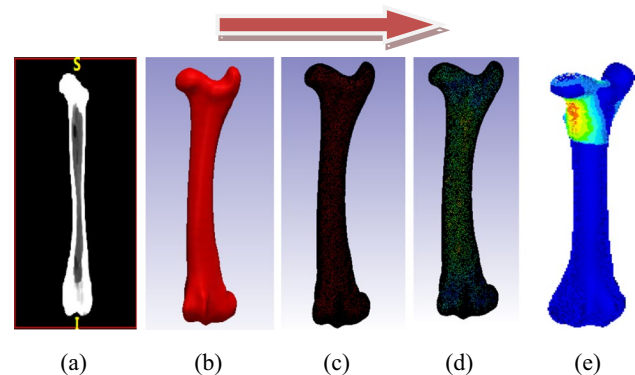


**Fig. 2** Steps to create three-dimensional FE femur bone model from CT scan image: **a** CT scan image **b** 3D model **c** meshing **d** material model **e** FE model



**Table 3** Image-based FEA for predicting biomechanical properties of femur bone

Loading config.	Image technique	FE model	Bone tilting angles	Failure criteria	Biomechanical properties	Reference
Stance	QCT scan	Heterogeneous	20°	–	FL	Hambliet al. [13]
Stance	CT scan	Nonlinear isotropic	0°	–	FL	Sas et al. [24]
Stance	CT scan	Linear, isotropic	8°	PS	$\sigma, \epsilon, FL$	Ota et al. [25]
Stance	CT scan	Isotropic, orthotropic, linear elastic	–	VM, PS	$\sigma$	Fonseca et al. [26]
Stance	CT scan	Isotropic, homogeneous, linear elastic	15°, 8°, 20°	PSt	$\epsilon$	Levadnyi et al. [27]
Stance	–	Isotropic, homogeneous, linear elastic	–	PSt	$\epsilon, d$	Polgar et al. [28]
Stance	CT scan	Isotropic, homogeneous, linear elastic	0°	MSt	$\epsilon$	Aziz et al. [29]
Stance	CT scan	Isotropic	20°	DE	FL	Keyak et al. [48]
Stance	CT scan	Anisotropic, orthotropic	20°	–	FP, FL, $d$	Hambli et al. [49]
Stance	CT scan	Isotropic, orthotropic	20°	–	FP	Bettameret al. [50]
Stance	CT scan	Isotropic, inhomogeneous	20°	VM	$\epsilon, FL, d$	Bettamer et al. [51]
Stance, Fall	MDCT scan	Isotropic, inhomogeneous	7°	PS, PSt	$\sigma, \epsilon$	Liebl et al. [52]
Stance	CT scan	Isotropic, anisotropic	0°, 15°, 20°	VM	$\sigma, \epsilon$	Painkra et al. [53]
Stance	CT scan	Isotropic	0°	VM, PS	$\sigma, d$	Chethan et al. [54]
Stance	CT scan	Isotropic, orthotropic	0°	PS	$\sigma, \epsilon$	Antonioet al. [55]
Stance	CT scan	Isotropic, orthotropic	12°	VM	$\sigma, d$	Peng et al. [56]
Stance, Fall	Laser scan	Linear, isotropic	0°	MS	$\sigma, FL$	Mughal et al. [63]
Stance	CT scan	Isotropic	0°	VM	$\sigma, d$	Kumar et al. [81, 82]
Stance	Laser scan	Orthotropic	0°, 90°	VM	$\sigma, \epsilon, d$	Dey et al. [83]
Stance	CT scan	–	–	VM	$\sigma$	Reddy et al. [84]
Stance	MDCT scan	Isotropic	0°	VM	$\sigma, \epsilon$	Mathukumar et al. [86]
Stance	CT scan	Inhomogeneous	3°, 8°, 24°	PSt	$\epsilon$	Schileoet al. [87]

*PSt*—Principal strain, *PS*—principal stress, *MSt*—maximum strain, *VM*—Von-mises, *DE*—distortion energy, *MS*—maximum stress, *FL*—fracture load, *FP*—fracture patterns

$\sigma$  = Stress,  $\epsilon$  = Strain,  $d$  = Displacement

### Comparison of Experimental and Numerical Model to Predict Biomechanical Properties

It is necessary to compare the biomechanical properties obtained from FEM and the experimental method for standardization and validation. However, the accurate image-based finite element model can be a noninvasive, fast and cost-effective method. The review represents some collective studies of the available literature that mainly provide the data on the errors/deviations (%) to investigate the biomechanical properties. Therefore, available studies have been included in determining stresses and strains using FEM and experimental methods to validate the femur bone. However, a significant deviation was observed in the range of 7–46.24% in stresses [53, 86, 89] and –127 to 120% in strains [43, 76, 86, 90–93].

On the other hand, another biomechanical characteristic, a fracture load, shows deviations in the range of 4.7–76.19%

[25, 52, 58, 59, 61, 77, 94]. This significant difference may be occurred due to some challenges in experimental analysis, such as mounting and acquiring the data from strain gauges, the accuracy of displacement rate, bone inclination and fracture load. In addition, a few challenges are observed in finite element analysis, such as constructing a geometrical model, generating the mesh, and assigning material properties and boundary conditions according to the loading application. Thus, there is a need to focus on increasing the accuracy to obtain the biomechanical properties of femur bone.

### Conclusions

This paper has described in detail about biomechanical properties of the femur bone under various physiological conditions. In addition, the functionality of the image-based FE model and its biomedical relevance has been discussed.

Besides, this study emphasizes that the noninvasive FE analysis of biomechanical properties will be increasingly used in designing and developing orthopaedic implants/fixations of the femur bone. However, the study compared and observed significant errors/deviations in the experimental and FE model. Moreover, this review study summarizes the different biomechanical properties by considering various loading conditions and FE model. It has also demonstrated more insights into biomechanical issues related to the fracture of femur bone. However, further investigations are needed to establish a standard procedure for femur bone testing and validation of the procedure to improve the accuracy of biomechanical properties. In the future, it is necessary to give more emphasis to the image-based FEM than the experimental method due to its flexibility. This review study also suggests using various advanced computing facilities like Simpleware ScanIP, 3D Doctor, Materialise Mimics and 3D Slicer use for creating effective and accurate 3D models from medical image scan data required for finite element analysis. In addition, researchers can incorporate other different anatomical conditions, such as bone inclinations and displacement rates, under different loading configurations.

**Acknowledgements** This article is the extended version of the selected presented papers during the International Conference on "Progressive Research in Industrial & Mechanical Engineering" (PRIME-2021).

**Funding** The authors did not receive support from any organization for the submitted work. No funding was received to assist with the preparation of this manuscript. No funding was received for conducting this study.

#### Declarations

**Conflict of interest** The authors declare that they have no competing interests.

## References

1. T.M. Keaveny, E.F. Morgan, O.C. Yeh, *Bone Mechanics, Biomedical Engineering and Design Handbook*, vol. 1, 2nd edn. (McGraw-Hill, New York, 2004)
2. R.A. Gujar, H.N. Warhatkar, Estimation of mass apparent density and Young's modulus of femoral neck-head region. *J. Med. Eng. Technol.* **44**(7), 378–388 (2020)
3. M.C. Vera, J.L. Ferretti, V. Abdala, G.R. COUNTRY, Biomechanical properties of anuran long bones: correlations with locomotor modes and habitat use. *J. Anat.* **236**(6), 1112–1125 (2020)
4. A.N. Nautiyal, P.K.S. Nain, P. Kumar, Study of knee-joint mechanism before implanting a knee prosthesis by modeling and finite element analysis of knee-joint bones. *Int. J. Adv. Mech. Eng.* **4**(7), 721–727 (2014)
5. A.E. Yousif, M.Y. Aziz, Biomechanical analysis of the human femur bone during normal walking and standing up. *IOSR J. Eng.* **2**(8), 13–19 (2012)
6. M. Toth-Tascau, L. Rusu, C. Toader, Biomechanical behavior of implanted long bones. *Annals of the Oradea University. Fascicle Manag. Technol. Eng.* **2**, 283–288 (2010)
7. H. Mohammed, R. Fazlur, Y. Mohammed, Z. Syed, P. Shanawaz, Y. Tajuddin, Hybrid polymer matrix composites for biomedical applications. *Int. J. Mod. Eng. Res.* **3**(2), 970–979 (2013)
8. C. Cooper, G. Champion, L.J. Melton, Hip fractures in the elderly: a world-wide projection. *Osteoporos. Int.* **2**, 285–289 (1992)
9. A. Svedbom, E. Hernlund, M. Ivergård, J. Compston, C. Cooper, J. Stenmark, E.V. McCloskey, B. Jönsson, J.A. Kanis, Osteoporosis in the European Union: a compendium of country-specific reports. *Arch. Osteoporos.* (2013). <https://doi.org/10.1007/s11657-013-0137-0>
10. S. Rath, L. Yadav, A. Tewari, T. Chantler, M. Woodward, P. Kotwal et al., Management of older adults with hip fractures in India: a mixed methods study of current practice, barriers and facilitators, with recommendations to improve care pathways. *Arch. Osteoporos.* **12**(55), 1–13 (2017)
11. S.M. Snyder, E. Schneider, Estimation of mechanical properties of cortical bone by computed tomography. *J. Orthop. Res.* **9**(3), 422–431 (1991)
12. G.J. Adams, R.B. Cook, J.R. Hutchinson, P. Zioupos, Bone apparent and material densities examined by cone beam computed tomography and the archimedes technique: comparison of the two methods and their results. *Front. Mech. Eng.* **3**(23), 1–9 (2018)
13. R. Hambli, S. Allaoui, A robust 3D finite element simulation of human proximal femur progressive fracture under stance load with experimental validation. *Ann. Biomed. Eng.* **41**(12), 2515–2527 (2013)
14. M. Ridzwan, C. Sukjamsri, B. Pal, R.J. van Arkel, A. Bell, M. Khanna, A. Baskaradas, R. Abel, O. Boughton, J. Cobb, U.N. Hansen, Femoral fracture type can be predicted from femoral structure: a finite element study validated by digital volume correlation experiments. *J. Orthop. Res.* **36**(3), 993–1001 (2017)
15. P. Ducheynet, L. Heymans, M. Martens, E. Aernoudt, P.D. Meester, J.C. Mulier, The mechanical behaviour of intracondylar cancellous bone of the femur at different loading rates. *J. Biomech.* **10**, 747–762 (1977)
16. E.F. Morgan, H.H. Bayraktar, T.M. Keaveny, Trabecular bone modulus–density relationships depend on anatomic site. *J. Biomech.* **36**, 897–904 (2003)
17. S.I. Esses, J.C. Lotz, W.C. Hayes, Biomechanical properties of the proximal femur determined in vitro by single-energy quantitative computed tomography. *J. Bone Miner. Res.* **4**(5), 715–722 (1989)
18. J.C. Lotz, T.N. Gerhart, W.C. Hayes, Mechanical properties of trabecular bone from the proximal femur: a quantitative CT study. *J. Comput. Assist. Tomograp.* **14**(1), 107–114 (1990)
19. W.C. Hayes, S.J. Piazza, P. Zysset, Biomechanics of fracture risk prediction of the hip and spine by quantitative computed tomography. *Radiol. Clin. North Am.* **29**(1), 1–18 (1991)
20. C.H. Turner, J. Rho, Y. Takano, T.Y. Tsui, G.M. Pharr, The elastic properties of trabecular and cortical bone tissues are similar: results from two microscopic measurement techniques. *J. Biomech.* **32**, 437–441 (1999)
21. H.H. Bayraktar, E.F. Morgan, G.L. Niebur, G.E. Morris, E.K. Wong, T.M. Keaveny, Comparison of the elastic and yield properties of human femoral trabecular and cortical bone tissue. *J. Biomech.* **37**, 27–35 (2004)
22. J.D. Currey, J. Foreman, I. Laketic, J. Mitchell, D.E. Pegg, G.C. Reilly, Effects of ionizing radiation on the mechanical properties of human bone. *J. Orthop. Res.* **15**, 111–117 (1997)
23. J.Y. Rho, R.B. Ashman, C.H. Turner, Young's modulus of trabecular and cortical bone material: ultrasonic and microtensile measurements. *J. Biomech.* **26**, 111–119 (1993)

24. A. Sas, N. Ohs, E. Tanck, G.H. van Lenthe, Nonlinear voxel-based finite element model for strength assessment of healthy and metastatic proximal femurs. *Bone Rep.* **12**, 100263 (2020)
25. T. Ota, I. Yamamoto, R. Morita, Fracture simulation of the femoral bone using the finite-element method: how a fracture initiates and proceeds. *J. Bone Miner. Metab.* **17**, 108–112 (1999)
26. E.M.M. Fonseca, M.J. Lima, L.M.S. Barreira, Human femur assessment using isotropic and orthotropic materials dependent of bone density. in 3rd International Conference on Integrity, Reliability and Failure, 20–24 July, Porto/Portugal, (2009), pp. 1–10
27. I. Leivadnyi, J. Awrejcewicz, Y. Zhang, Y. Gu, Comparison of femur strain under different loading scenarios: experimental testing. *J. Eng. Med.* **235**(1), 17–27 (2021)
28. K. Polgar, H.S. Gill, M. Viceconti, D.W. Murray, J.J. O'Connor, Strain distribution within the human femur due to physiological and simplified loading: finite element analysis using the muscle standardized femur model. *J. Eng. Med.* **217**(3), 173–189 (2003)
29. A.U.A. Aziz, H.S. Gan, A.K. Nasution, M.R.A. Kadir, M.H. Ramlee, Development and verification of three-dimensional model of femoral bone: finite element analysis. *J. Phys. Conf. Series* **1372**, 012014 (2019)
30. J.Y. Rho, M.C. Hobatho, R.B. Ashman, Relations of mechanical properties to density and CT numbers in human Bone. *Med. Eng. Phys.* **17**(5), 347–355 (1995)
31. P.K. Zysset, X.E. Guo, C.E. Hoffler, K.E. Moore, S.A. Goldstein, Elastic modulus and hardness of cortical and trabecular bone lamellae measured by nanoindentation in the human femur. *J. Biomech.* **32**, 1005–1012 (1999)
32. J.Y. Rho, T.Y. Tsui, G.M. Pharr, Elastic properties of human cortical and trabecular lamellar bone measured by nanoindentation. *Biomaterials* **18**, 1325–1330 (1997)
33. X. Li, M. Viceconti, M.C. Cohen, G.C. Reilly, M.J. Carre, A.C. Offiah, Developing CT based computational models of pediatric femurs. *J. Biomech.* **48**, 2034–2040 (2015)
34. E. Schiello, E. Dall'Ara, F. Taddei, A. Malandrino, T. Schotkamp, M. Baleani, M. Viceconti, An accurate estimation of bone density improves the accuracy of subject-specific finite element models. *J. Biomech.* **41**, 2483–2491 (2008)
35. B. Helgason, E. Perilli, E. Schileo, F. Taddei, S. Brynjolfsson, M. Viceconti, Mathematical relationships between bone density and mechanical properties: a literature review. *Clin. Biomech.* **23**, 135–146 (2008)
36. D. Zang, D.D. Arola, J.A. Rouland, Evaluating the elastic modulus of bone using electronic speckle pattern interferometry. *Exp. Tech.* **25**(5), 32–34 (2001)
37. A. Sitzer, R. Wendlandt, J. Barkhausen, A. Kovacs, I. Weyers, Ap. Schulz, A P Schulz (2012) Determination of material properties related to quantitative CT in human femoral bone for patient specific finite element analysis-a comparison of material laws. *Webmed Cent. Orthop.* **3**(3), 1–11 (2012)
38. L. Cyganik, M. Binkowski, G. Kokot, T. Rusin, P. Popik, F. Bolechała, R. Nowak, Z. Wróbel, A. John, Prediction of elastic modulus of trabeculae in microscale using macro-scale's relationships between bone density and mechanical properties. *J. Mech. Behav. Biomed. Mater.* **36**, 120–134 (2014)
39. G.L. Niebur, M.L. Feldstein, J.C. Yuen, T.J. Chen, T.M. Keaveny, High-resolution finite element models with tissue strength asymmetry accurately predict failure of trabecular bone. *J. Biomech.* **33**, 1575–1583 (2000)
40. O. Brennan, O.D. Kennedy, T.C. Lee, S.M. Rackard, F.J. O'Brien, Biomechanical properties across trabeculae from the proximal femur of normal and ovariectomised sheep. *J. Biomech.* **42**, 498–503 (2009)
41. J.C. Lotz, E.J. Cheal, W.C. Hayes, Fracture prediction for the proximal femur using finite element models: part I-linear analysis. *J. Biomech. Eng.* **113**(4), 353–360 (1991)
42. D.C. Wirtz, N. Schiffers, T. Pandorf, Critical evaluation of known bone material properties to realize anisotropic FE-simulation of the proximal femur. *J. Biomech.* **33**(10), 1325–1330 (2000)
43. Z. Yosibash, R. Padan, L. Joskowicz, C. Milgrom, A CT-based high-order finite element analysis of the human proximal femur compared to in-vitro experiments. *J. Biomech. Eng.* **129**, 297–309 (2007)
44. M.W.M. Koo, K.H. Yang, P. Begeman, M. Hammami, W.W.K. Koo, Prediction of bone strength in growing animals using noninvasive bone mass measurements. *Calcif. Tissue Int.* **68**, 230–234 (2001)
45. J.H. Keyak, T.S. Kaneko, S.A. Rossi, M.R. Pejcić, J. Tehranzadeh, H.B. Skinner, Predicting the strength of femoral shafts with and without metastatic lesions. *Clin. Orthop. Relat. Res.* **439**, 161–170 (2005)
46. K. Mckinsey, Investigating the likelihood of pediatric femur fracture due to falls through finite element analysis. *Electronic Theses and Dissertations, University of Louisville.*5 (2018)
47. Z.S. Ferlengez, J.B. Pljakic, O.D. Kennedy, C.J. Philemon, M.B. Schaffler, Structural and mechanical repair of diffuse damage in cortical bone in vivo. *J. Bone Miner. Res.* **29**(12), 2537–2544 (2014)
48. J.H. Keyak, Y. Falkinstein, Comparison of in situ and in vitro CT scan-based finite element model predictions of proximal femoral fracture load. *Med. Eng. Phys.* **25**, 781–787 (2003)
49. R. Hambli, A. Bettamer, S. Allaoui, Finite element prediction of proximal femur fracture pattern based on orthotropic behaviour law coupled to quasi-brittle damage. *Med. Eng. Phys.* **34**, 202–210 (2012)
50. A. Bettamer, R. Hambli, S. Allaoui, A. Barkaoui, A. El Hraiech, R.R. Jennane, Proximal human femur fracture assessment using isotropic and orthotropic materials: A comparative FE-study using quasi brittle damage models. *European Congress on Computational Methods in Applied Sciences and Engineering (ECCOMAS 2012)*. September 10–14, Vienna, Austria, (2012), pp. 1–9
51. A. Bettamer, R. Hambli, S. Allaoui, A.A. Imjabber, Using visual image measurements to validate a novel finite element model of crack propagation and fracture patterns of proximal femur. *Comput. Methods Biomech. Biomed. Eng. Imaging Vis.* **5**(4), 251–262 (2015)
52. H. Liebl, E.G. Garcia, F. Holzner, P.B. Noel, R. Burgkart, E.J. Rummeny, T. Baum, J.S. Bauer, In-vivo assessment of femoral bone strength using finite element analysis (FEA) based on routine MDCT imaging: a preliminary study on patients with vertebral fractures. *PLoS ONE* **10**(2), 1–15 (2015)
53. R. Painkra, S. Sanyal, A. Bit, An anisotropic analysis of human femur bone with walking posture: experimental and numerical analysis. *BioNanoScience.* **8**, 1054–1064 (2018)
54. K.N. Chethan, S.N. Bhat, M. Zuber, S.B. Shenoy, Patient-specific static structural analysis of femur bone of different lengths. *Open Biomed. Eng. J.* **12**(1), 108–114 (2018)
55. T.S. Antonio, M. Ciaccia, C. Müller-Karger, E. Casanova, Orientation of orthotropic material properties in a femur FE model: a method based on the principal stresses directions. *Med. Eng. Phys.* **34**, 914–919 (2012)
56. L. Peng, J. Bai, X. Zeng, Y. Zhou, Comparison of isotropic and orthotropic material property assignments on femoral finite element models under two loading conditions. *Med. Eng. Phys.* **28**, 227–233 (2006)
57. M.R. Zarrinkalam, H. Beard, C.G. Schultz, R.J. Moore, Validation of the sheep as a large animal model for the study of vertebral osteoporosis. *Eur. Spine J.* **18**, 244–253 (2009)
58. Z. Yosibash, D. Tal, N. Trabelsi, Predicting the yield of the proximal femur using high-order finite-element analysis with inhomogeneous orthotropic material properties. *Phil. Trans. R. Soc. A* **368**, 2707–2723 (2010)



59. M. Miura, J. Nakamura, Y. Matsuura, Y. Wako, T. Suzuki, S. Hagiwara, S. Orita, K. Inage, Y. Kawarai, M. Sugano, K. Nawata, S. Ohtori, Prediction of fracture load and stiffness of the proximal femur by CT-based specimen specific finite element analysis: cadaveric validation study. *BMC Musculoskeletal Disord* **18**(1), 536 (2017)
60. M. Bessho, I. Ohnishi, J. Matsuyama, T. Matsumoto, K. Imai, K. Nakamura, Prediction of strength and strain of the proximal femur by a CT-based finite element method. *J. Biomech.* **40**, 1745–1753 (2007)
61. E. Schileo, L. Balistreri, L. Grassi, L. Cristofolini, F. Taddei, To what extent can linear finite element models of human femora predict failure under stance and fall loading configurations? *J. Biomech.* **47**, 3531–3538 (2014)
62. E. Schileo, F. Taddei, L. Cristofolini, M. Viceconti, Subject-specific finite element models implementing a maximum principal strain criterion are able to estimate failure risk and fracture location on human femurs tested in vitro. *J. Biomech.* **41**, 356–367 (2008)
63. U.N. Mughal, H.A. Khawaja, M. Moatamedi, Finite element analysis of human femur bone. *Int. J. Multiphysics* **9**(2), 101–108 (2015)
64. J.H. Keyak, H.B. Skinner, J.A. Fleming, Effect of force direction on femoral fracture load for two types of loading conditions. *J. Orthop. Res. Off. Publ. Orthop. Res. Soc.* **19**(4), 539–544 (2001)
65. S. Gilchrist, P. Guy, P.A. Cripton, Development of an inertia-driven model of sideways fall for detailed study of femur fracture mechanics. *J. Biomech. Eng.* **135**(12), 121001 (2013)
66. L. Zani, L. Cristofolini, M.M. Juszczak, L. Grassi, M. Viceconti, A new paradigm for the in vitro simulation of sideways fall loading of the proximal human femur. *J. Mech. Med. Biol* **14**, 1450005 (2014)
67. H. Warhatkar, A. Chawla, S. Mukherjee, *Experimental study of variation between quasi-static and dynamic load deformation properties of bovine medial collateral ligaments* (SAE International, Warrendale, 2008)
68. L. Cristofolini, M. Juszczak, S. Martelli, F. Taddei, M. Viceconti, In vitro replication of spontaneous fractures of the proximal human femur. *J. Biomech.* **40**(13), 2837–2845 (2007)
69. M. Juszczak, L. Cristofolini, J. Kaniuk, E. Schileo, M. Viceconti, A novel method for determining the time and location of abrupt fracture initiation in bones. *J. Strain Anal. Eng. Des.* **45**, 481–493 (2010)
70. M.M. Juszczak, L. Cristofolini, M. Viceconti, The human proximal femur behaves linearly elastic up to failure under physiological loading conditions. *J. Biomech.* **44**(12), 2259–2266 (2011)
71. M.M. Juszczak, L. Cristofolini, M. Salvà, L. Zani, E. Schileo, M. Viceconti, Accurate in vitro identification of fracture onset in bones: failure mechanism of the proximal human femur. *J. Biomech.* **46**(1), 158–164 (2013)
72. J.H. Keyak, Relationships between femoral fracture loads for two load configurations. *J. Biomech.* **33**(4), 499–502 (2000)
73. L. Cristofolini, M. Juszczak, F. Taddei, M. Viceconti, Strain distribution in the proximal human femoral metaphysis. *Proc. Inst. Mech. Eng. Part H J. Eng. Med.* **223**(3), 273–288 (2009)
74. L. Duchemin, D. Mitton, E. Jolivet, V. Bousson, J. Laredo, W. Skalli, An anatomical subject-specific FE-model for hip fracture load prediction. *Comput. Methods Biomech. Biomed. Engin.* **11**(2), 105–111 (2008)
75. W. Schaasberg, T.J. van der Steenhoven, S.K. van de Velde, R.G. Nelissen, E.R. Valstar, Feasibility of osteosynthesis of fractured cadaveric hips following preventive elastomer femoroplasty. *Clin. Biomech. (Bristol, Avon)* **29**(7), 742–746 (2014)
76. N. Trabelsi, Z. Yoshibash, C. Wutte, P. Augat, S. Eberle, Patient-specific finite element analysis of the human femur—a double-blinded biomechanical validation. *J. Biomech.* **44**, 1666–1672 (2011)
77. R. Larrainzar-Garjio, J.R. Caeiro, M. Marco, E. Giner, M.H. Miguelez, Experimental validation of finite elements model in hip fracture and its applicability. *Rev. Esp. Cir. Ortop. Traumatol.* **63**(2), 146–154 (2019). (English ed.)
78. H. YueHuei, R.A. Draughen, *Mechanical testing of bone and bone implant interface*, 1st edn. (CRC Press, New York, 2000). <https://doi.org/10.1201/9781420073560>
79. F. Taddei, E. Schileo, B. Helgason, L. Cristofolini, M. Viceconti, The material mapping strategy influences the accuracy of CT-based finite element models of bones: an evaluation against experimental measurements. *Med. Eng. Phys.* **29**, 973–979 (2007)
80. M. Lengsfeld, J. Schmitt, P. Alter, J. Kaminsky, R. Leppek, Comparison of geometry-based and CT voxel-based finite element modeling and experimental validation. *Med. Eng. Phys.* **20**, 515–522 (1998)
81. N.K.C. Kumar, T. Tandon, P. Silori, A. Shaikh, Biomechanical stress analysis of a human femur bone using ANSYS. *Mater. Today Proc.* **2**(4–5), 2115–2120 (2015)
82. N.K.C. Kumar, N. Griya, A. Shaikh, V. Chaudhr, S. Chavadaki, Structural analysis of femur bone to predict the suitable alternative material. *Mater. Today Proc.* **26**(2), 364–368 (2020)
83. S. Dey, Finite element analysis of human femur bone for axial and bending load application on its head. in *Proceedings of the 5th International Conference on Engineering Research, Innovation and Education (ICERIE)*. 25–27 January, Sylhet, Bangladesh, (2019), pp. 1–6
84. M.V. Reddy, B.K.C. Ganes, K.C.K. Bharathi, P. Chittibabu, J. Osteoporos. *Phys. Act.* **4**(3), 1000180 (2016)
85. H. Yang, X. Ma, T. Guo, Some factors that affect the comparison between isotropic and orthotropic inhomogeneous finite element material models of femur. *Med. Eng. Phys.* **32**, 553–560 (2010)
86. S. Mathukumar, V.A. Nagarajan, A. Radhakrishnan, Analysis and validation of femur bone data using finite element method under static load condition. *J. Mech. Eng. Sci.* **233**(16), 5547–5555 (2019)
87. E. Schileo, F. Taddei, A. Malandrino, L. Cristofolini, M. Viceconti, Subject-specific finite element models can accurately predict strain levels in long bones. *J. Biomech.* **40**, 2982–2989 (2007)
88. R.A. Gujar, H.N. Warhatkar, In vitro estimation of fracture load and strain in sheep femur bone: experimental approach. *Mater. Today Proc.* **44**(5), 3792–3797 (2021)
89. I. Manarvi, An investigation of animal and human bones for predicting probable location of fractures. in *38<sup>th</sup> Annual International Conference of the IEEE Engineering in Medicine and Biology Society (EMBC)*. 978-1-4577-0220-4:2194-97 (Orlando, FL, 2016)
90. D. Kluess, E. Soodmand, A. Lorenz, D. Pahr, M. Schwarze, R. Cichon, P.A. Varady, S. Harrman, B. Buchmeier, C. Schroder, S. Lehner, M. Keibach, A round-robin finite element analysis of human femur mechanics between seven participating laboratories with experimental validation. *Comput. Methods Biomech. Biomed. Eng.* **22**(12), 1020–1031 (2019)
91. V. Filardi, D. Milardi, Experimental strain analysis on the entire bony leg compared with FE analysis. *J. Orthop.* **14**, 115–122 (2017)
92. R. Montanini, V. Filardi, In vitro biomechanical evaluation of antegrade femoral nailing at early and late postoperative stages. *Med. Eng. Phys.* **32**, 889–897 (2010)
93. T.L. Alexandra, D.M. Cristian, H. Mihail, B.A. Loan, Experimental validation of a finite element model of an osteoporotic human femoral bone using strain gauge measurement. *Appl. Mech. Mater. Trans. Tech. Publ.* **658**, 513–519 (2014)
94. M. Mirzaei, S. Samiezadeh, A. Khodadadi, M.R. Ghazavi, Finite element prediction and experimental verification of the failure

pattern of proximal femur using quantitative computed tomography images. *Int. J. Biomed. Biol. Eng.* **6**(6), 208–214 (2012)

**Publisher's Note** Springer Nature remains neutral with regard to jurisdictional claims in published maps and institutional affiliations.

Springer Nature or its licensor (e.g. a society or other partner) holds exclusive rights to this article under a publishing agreement with the author(s) or other rightsholder(s); author self-archiving of the accepted manuscript version of this article is solely governed by the terms of such publishing agreement and applicable law.